

Development of Zirconium Thin Films by Pulsed Direct Current Magnetron Sputtering: Effect of Pulsed Parameters

Akash Singh*, P. Kuppusami¹, R. Thirumurugesan, V. Ganesan² and E. Mohandas

*Physical Metallurgy Group, Indira Gandhi Centre for Atomic Research, Kalpakkam-603 102.

¹Centre for Nanoscience and Nanotechnology, Sathyabama University, Chennai-600 119

²UGC-DAE Consortium for Scientific Research, University Campus, Khandwa Road, Indore.

Abstract

This paper characterizes phases present in thin Zr films at 773 K of substrate temperature. The effect of pulsed parameters such as pulse frequency, duty cycle and pulse power during the deposition of Zr film on Si(100) at the substrate temperature of 773 K has been studied. Formation of α -phase of zirconium was noticed with (001) preferred orientation at 773 K. Preferred orientation was found to be influenced by the pulse parameters. It is noticed that crystallite size decreased with increasing frequency and duty cycle, whereas it increased with increasing pulse power. Nanoindentation measurements indicated that the hardness of the films was in the range 4-8 GPa as a function of pulsed parameters.

Keywords: Magnetron sputtering, Zirconium, Microstructure, Texture, Hardness

I. INTRODUCTION

Zirconium and its alloys in bulk and thin film forms are widely used in nuclear industry and in reprocessing plants owing to their exceptional resistance to corrosion [1]. Zirconium is a IV-group transition element and has superior corrosion resistance against concentrated nitric acid at elevated temperature. It is used as a material for chemical plants to produce nitric acid or spent nuclear fuel reprocessing plants. Good refractory properties of zirconium oxides and high hardness, electrical conductivity of zirconium nitrides provide wide scope for these materials for industrial applications [2-7].

Zirconium oxides and nitrides are also widely employed in industry because of their interesting properties: good refractory properties for oxides and high hardness and electrical conductivity for nitrides [8]. In that case, knowledge of the initial Zr film microstructure is of prime importance as it can influence on the reaction and the final product. The initial structure may be strongly dependent on the conditions used for the deposition process especially when using non-equilibrium growth mechanisms occurring with highly energetic ion

bombardment. Thin films of zirconium oxides and nitrides can be prepared by the treatment of Zr thin films under oxidizing or nitriding atmospheres [9]. Zr based hard coatings are of great interest in a number of technological and medical implant [10] applications due to their improved tribological, corrosion, mechanical and physical properties. Also, polycrystalline zirconium films are used in thin multilayer for various applications such as metallic super lattice formation [11-13]. Zirconium thin films have been suggested as a diffusion barrier between U-Mo fuel and aluminum cladding in order to maintain the integrity of the fuel plates and to prevent fuel plate swelling and possible rupture during reactor operation [14]. Zirconium and titanium films have been also deposited on copper substrate to produce neutrons through deuterium-deuterium (D-D) and deuterium-tritium (D-T) reactions for neutron generator applications [15-16].

Sputtering is the most popular metal thin film deposition process. There exist commercially available codes [17-18] enabling the user to calculate the distribution of sputtered material at the substrate surface. Performing DC magnetron sputtering from a pure metal target in an ambient of Ar, the presence of oxygen in the

processing chamber may result in some oxidation of the metal target surface. The thin oxide coating at the target may be charged by the bombarding ions. This will result in micro arcing at this surface. During such arcing micro particles may be formed resulting in a coating with undesirable inclusions of micro particles. To overcome this problem it has become quite popular to use a pulsed direct current (DC) power in the form of high negative pulses interrupted by small positive pulses (arc suppression) [19-20]. In this way the charge at the oxide surface on the target may be neutralized by attracting electrons during the positive part of the duty cycle. It has been shown that properly matched positive and negative pulses may allow for arc free reactive sputter deposition of insulating materials from pure metal targets. Therefore, it is necessary to select the right power source parameters during the synthesis of these films.

The effect of substrate temperature on the microstructure of Zr films at constant pulsed parameters has been reported and well grown hexagon shaped crystallites have been noticed at the substrate temperature of 773 K [21]. These films were deposited at 100 kHz of pulse frequency, 20 % of duty cycle and 100 W of pulse power. However the effect of pulsed parameters was not fully understood. In this work, the effect of pulse frequency, duty cycle and pulse power on the microstructure of Zr films deposited at 773 K is investigated. In the present study, a systematic investigation on the effect of pulsed parameters to achieve good quality films of Zr on titanium modified austenitic stainless steel (D-9 alloy) substrates is reported.

II. MATERIAL AND METHODS

Zirconium target of 99.9% purity was used to deposit zirconium films of thickness in the range 1.2–1.5 μm on to D-9 alloy substrates at 773 K . D-9 alloy (whose composition is given in Table 1) is used as a clad material in breeder reactors. A zirconium target (purity better than 99.9%) of 76 mm diameter and 2 mm thickness was used to deposit zirconium films of thickness of $\sim 1.5 \mu\text{m}$ on to titanium modified austenitic stainless steel (D-9 alloy)

D-9 alloy (whose composition is given in Table 1) is used as a clad material in breeder reactors. The sputtering was carried out using a Mighty Mak US sputtering gun of 3 inch diameter in a custom built magnetron sputtering system A RPG-50 asymmetric bipolar pulsed DC power supply (MKS instruments, USA) was used as the electrical power source for the sputter deposition. The substrate temperature was kept constant at 773 K using a halogen lamp (800W, 6.3 A) heater with a digital programmable temperature controller. The sputtering method has been reported earlier [21]. The deposition conditions and pulsed parameters used in the present investigations are given in Table 2. During the sputtering, negative pulses were applied to the target, and the duration of pulses can be adjusted by varying the duty cycle of the pulse. Duty cycle can be defined as the ratio of on time and total time of the pulse. Duty cycle in the range 10-40%, pulse frequency in the range 50-200 kHz and pulse power in the range 50-125 W were applied to study the effect of these parameters on the microstructure of Zr films.

Table 1. Chemical composition (wt.%) of titanium modified stainless steel (alloy D-9).

| Elem. | C | Ni | Cr | Mo | Ti | Si | Mn | S | P | Al | B | N | Fe |
|-------|------|------|------|-----|------|----------|-----|--------|-------|---------|--------|-------|-----|
| Wt. % | 0.05 | 14.9 | 14.7 | 2.2 | 0.18 | 0.6 5 | 1.3 | <0.005 | 0.008 | <0.0034 | 0.0015 | <0.04 | Bal |

Table 2. Experimental parameters for deposition of Zr thin films

| | |
|------------------------------|-------------------------|
| Base pressure | 8×10^{-4} Pa |
| Operating pressure | 7.5×10^{-1} Pa |
| Target voltage | 205–230 V |
| Substrate temperature | 773 K |
| Pulse power | 50-125 W |
| Duty cycle | 10-40% |
| Pulse frequency | 50-200 kHz |
| Argon flow rate | 50 sccm |
| Substrate to target distance | 60 mm |

The thickness of the films was measured using DEKTAK 6M-stylus profiler (Veeco, USA). Structural properties of the as deposited Zr films were characterized by X-ray diffraction (XRD). The XRD patterns were recorded in an INEL XRG – 3000 diffractometer with a glancing angle incidence (ω) of 5° using Cu K α radiation. The crystallite size was determined using the Scherrer formula. Texture coefficients (TC) of (0 0 2) and (1 0 1) reflections were determined from the intensities of Zr peaks. In general, the TC (Texture Coefficient) for any reflection can be determined using the following relation.

Texture Coefficient

$$(TC): \frac{I_m(hkl)}{I_o(hkl)} \dots\dots\dots (1)$$

$$\frac{1}{n} \sum \frac{I_m(hkl)}{I_o(hkl)}$$

where n, the number of peaks; I_m , the measured peak intensities of reflections of Zr films; and I_o , the respective peak intensities corresponding to the bulk Zr data from JCPDS File No. 05-0665. XL30 ESEM Philips scanning electron microscope (SEM) was used to analyze the surface morphology and composition of the films. Surface morphology of the films was also examined in an atomic force microscope (AFM) using Digital Instruments Inc., Nanoscope E, US in contact mode. The nanohardness measurements were carried out by means of a nanoindenter (CSM, Switzerland).

III RESULTS

A. The role of pulse frequency

Fig.1 (a) shows XRD patterns of Zr films deposited on D-9 alloy substrate at 773 K and at various pulse frequencies (50, 100, 150, 200 kHz) and at constant pulse power and duty cycle of 100 W and 20%, respectively. The Fig. 1 shows that films are polycrystalline in nature and all the reflections are from α -Zr. For the calculation of crystallite size, (002) and (101) reflections have been considered at different pulse frequencies and it is found that, the crystallite size decreases more rapidly above 100 kHz of pulse frequency (Fig.1(c)). The deposition rate also decreases as pulse frequency increases (Fig. 1 (b)). It is observed that initially the Zr film exhibit (002) preferred orientation (Fig. 2) but with increasing pulse frequency (101) becomes the preferred orientation.

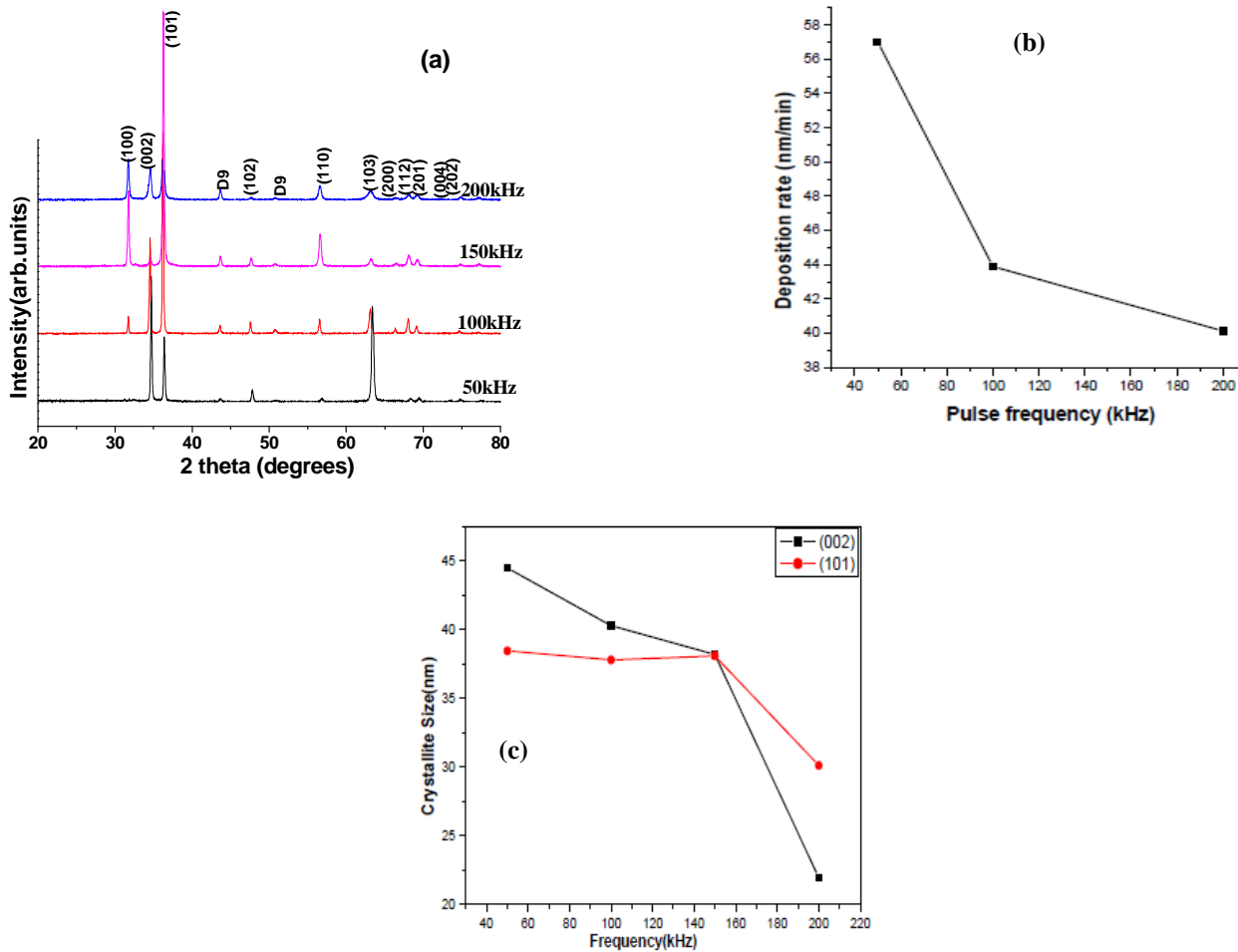


Fig. 1 (a) XRD pattern of Zr thin films as a function of pulse frequency, (b) Deposition rate and (c) Crystallite size versus pulse frequency.

Strain free lattice parameters ratios c/a for all Zr films deposited at different pulse frequency is found to be higher than the reported value of c/a in bulk. SEM (Fig. 3) and AFM (Fig. 4) images clearly show the similar variation of crystallite size with increasing pulse frequency.

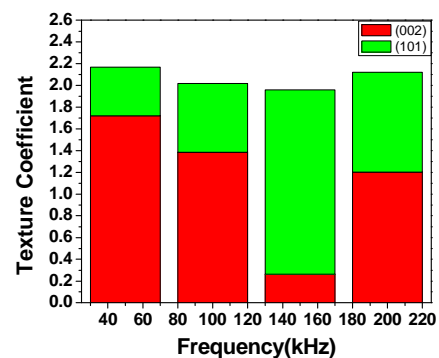


Fig.2 Texture coefficient versus pulse frequency

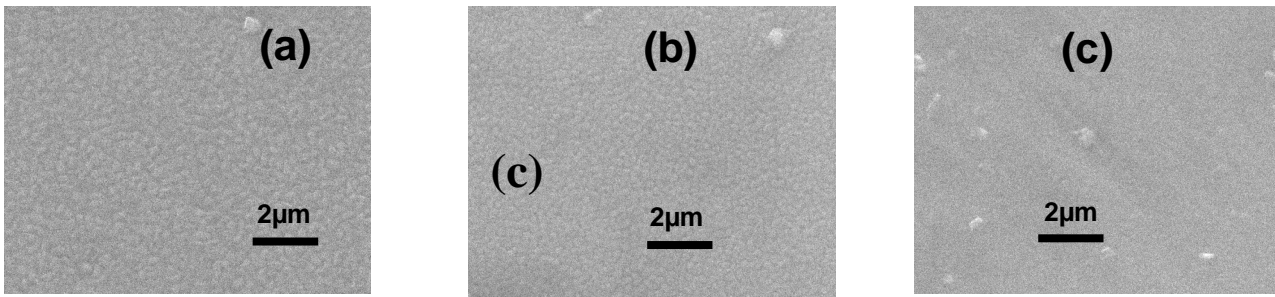


Fig. 3 SEM image of Zr films deposited at 773 K at pulse frequency of (a) 50, (b) 100 and (c) 200 kHz.

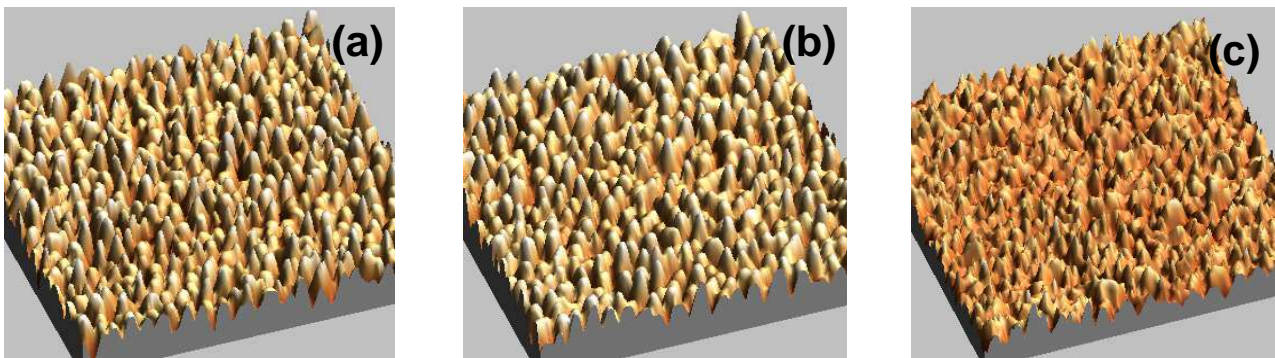


Fig. 4 AFM image (5 μm x 5 μm) of Zr films deposited at 773 K and at pulse frequency of (a) 50, (b) 100 and (c) 200 kHz

B. The role of duty cycle

Fig. 5 (a) shows XRD patterns of α -Zr films deposited on D-9 alloy substrate at 773 K and various duty cycles (10%, 20%, 30% and 40%) at constant pulse power of 100 W and constant pulse frequency of 100 kHz. It is noticed that all the reflections present in the XRD pattern belong to the α -hcp phase of Zr. The crystallite size was calculated using (002) reflection and is found to be decreasing with increasing pulse width. The XRD results also indicate that crystallinity decreases with the increase in the duty cycle (Fig. 5(c)). It is also noticed that the deposition rate increases with increase in duty cycle (Fig. 5 (b)). Crystallite size decreases from \sim 43 nm to 30

nm with increasing duty cycle from 10 to 40 %. It is observed that initially the Zr film exhibits (002) preferred orientation (Fig. 6) but with increasing duty cycle (101) becomes the preferred orientation. The anisotropic grain growth, thermal stress and texture of the grains are responsible for the evolution of three-dimensional hexagonal structures at higher duty cycle. The anisotropic grain growth may occur in Zr thin films due to factors such as preferred orientation of the grains, orientation-dependent grain boundary mobility and grain boundary free energy. AFM (Fig. 7) images clearly show the variation of crystallite size with increasing duty cycle. Surface roughness was also calculated and is found to be decreasing from 10 to 7 nm as a function of duty cycle

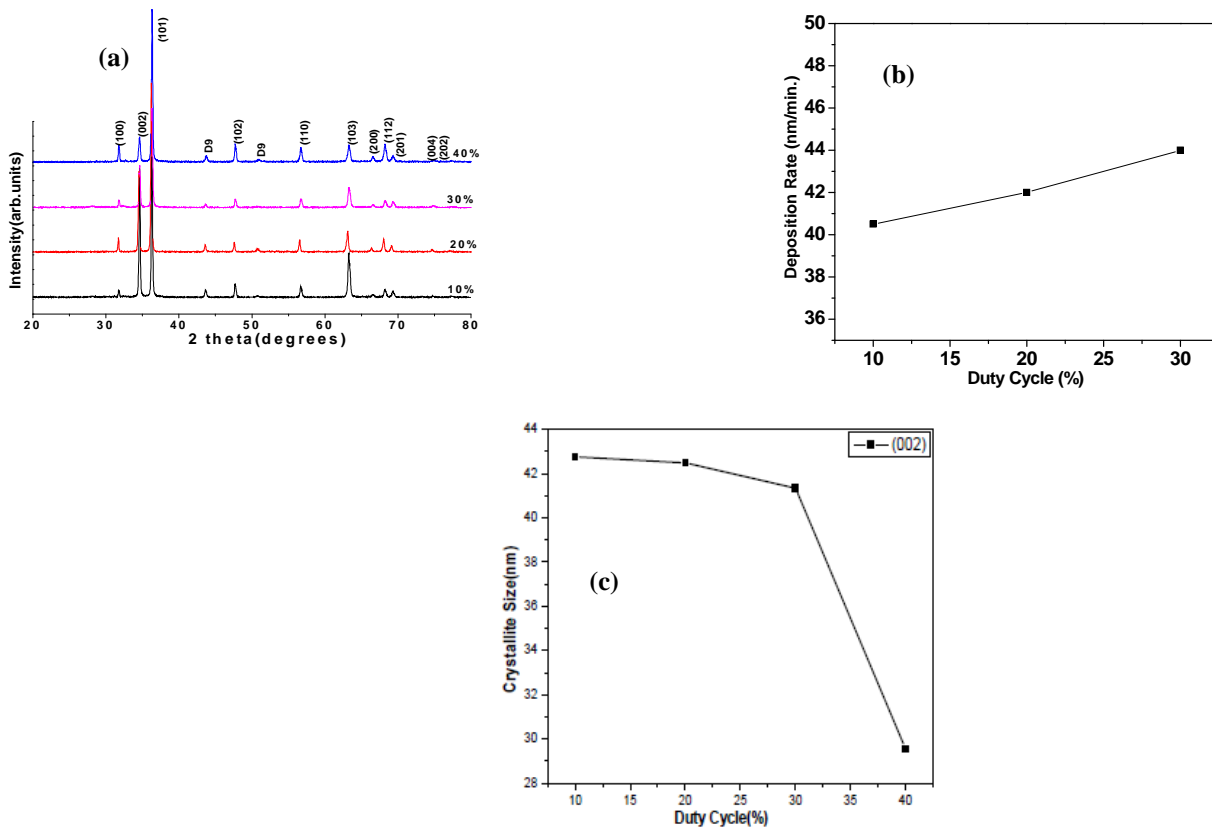


Fig. 5 (a) XRD pattern of Zr thin films as a function of pulse width, (b) Deposition rate and (c) Crystallite size versus duty cycle.

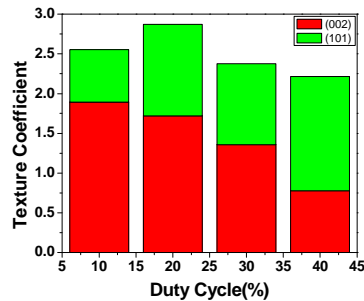


Fig 6 Variation of texture coefficient in Zr film deposited on D-9 alloy as a function of duty cycle

C. The role of pulse power

Fig. 8 (a) shows the XRD pattern of Zr thin films deposited on D-9 alloy substrate at 773 K, pulse power of 50, 75, 100 and 125 W constant frequency of 100 kHz and constant duty cycle of 20%. Fig. 8 (c) demonstrates the qualitative dependence of the crystallite size on the pulsed DC power. It is also noticed that the crystallite size and deposition rate (Fig.8 (b) & (c)) increases with

increasing power. Crystallite size was calculated using Scherrer's formula for the (002) and (101) reflections of the Zr pattern obtained as a function of different pulse power. For the Zr films deposited at 50, 75, 100 and 125 W, the corresponding crystallite size is $\sim 30, 35, 47$ and 62 nm respectively. It is observed that the Zr film exhibits (0 0 2) and (101) preferred orientation with increasing power (Fig. 9). AFM (Fig.10) images clearly show well grown crystallites at higher pulse power.

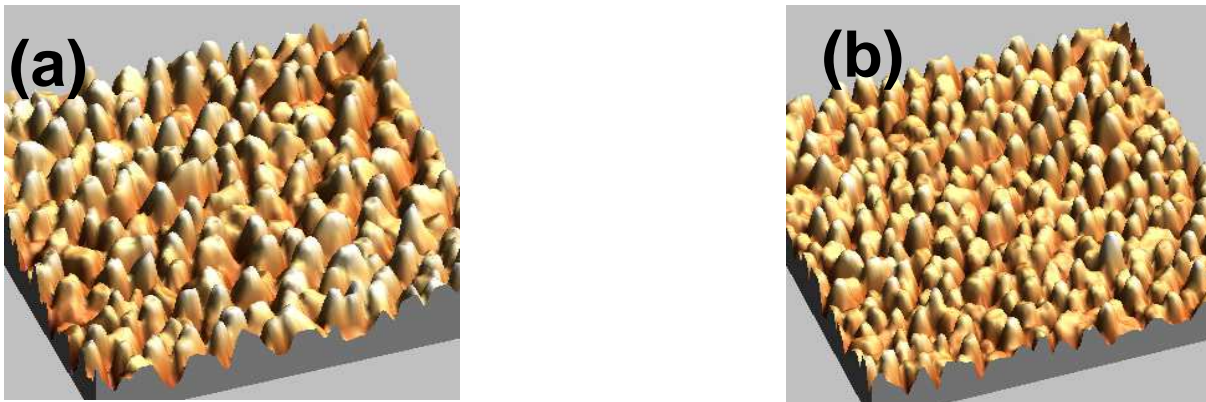


Fig. 7 AFM image (2 μm x 2 μm) of Zr films deposited at 773 K and at (a) 10% and (b) 30% of duty cycle

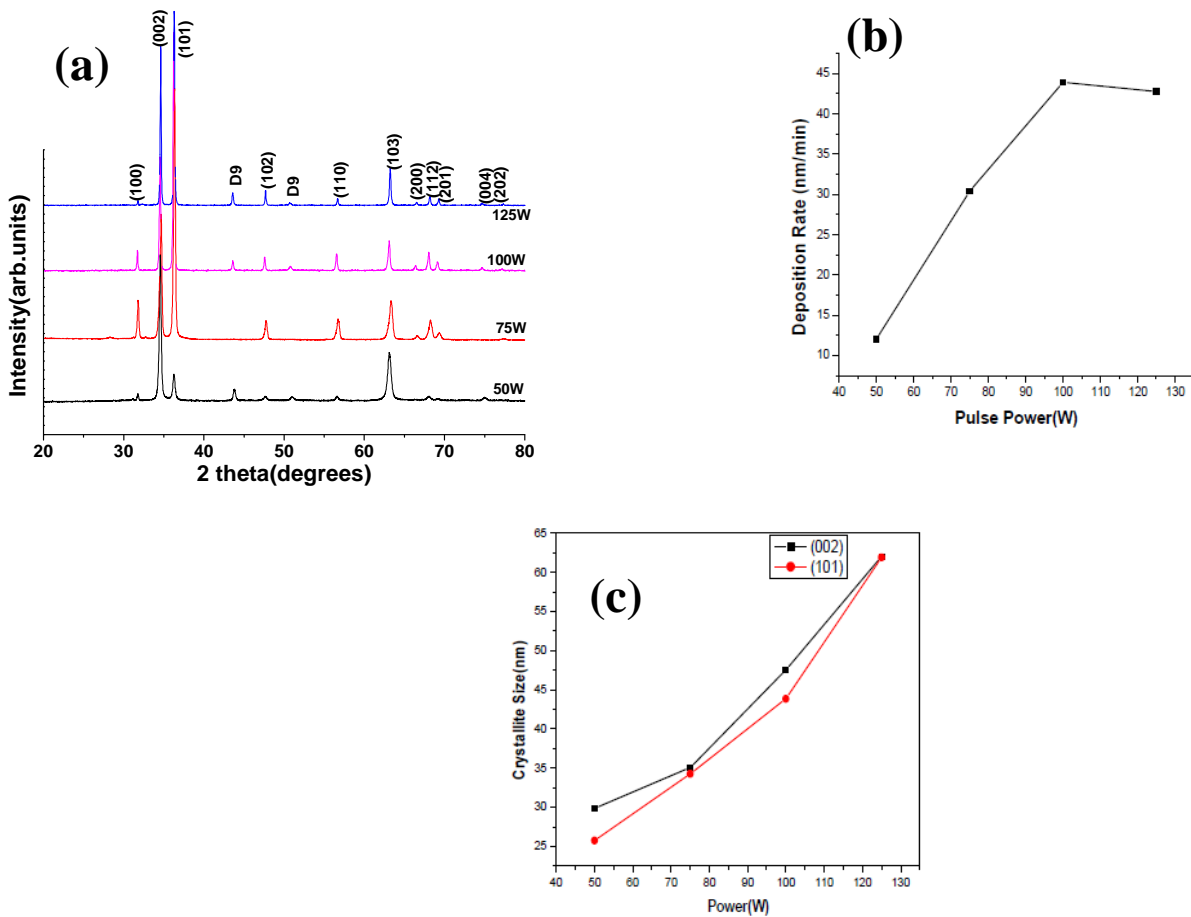


Fig. 8 (a) XRD pattern of Zr thin films as a function of pulse power, (b) Deposition rate and (c) Crystallite size versus pulse power.

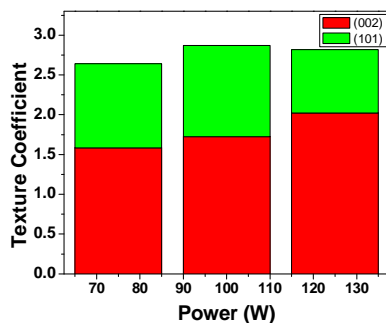


Fig. 9 Texture coefficients as a function of duty cycle

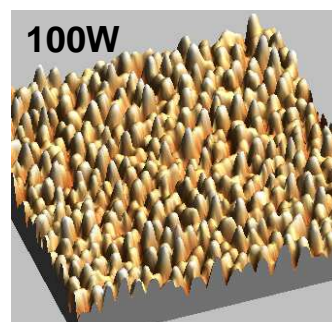
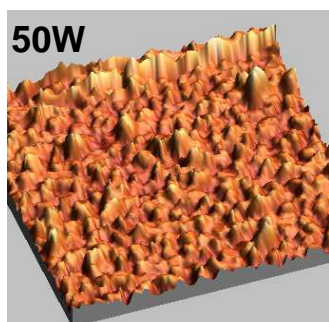


Fig. 10 AFM image (5 μm x 5 μm) of Zr films deposited at (a) 50 W, (b) 75 W and (c) 100 W of pulse power

D.Nanohardness of Zr thin films

In the present study film thickness was about 1.5 micrometer. Hardness was determined by nanoindentation and to avoid the contributions from the substrate the indentation depth performed ranged from 100 to 150nm to ensure the correctness of this method for measuring mechanical properties of the thin films. For measuring hardness and modulus using the nanoindentation method with a Berkovich indenter, indentation load, P, with displacement, h, is continuously recorded during one complete cycle of loading and unloading [22]. Hardness represents a complex combination of the deformation characteristics of thin films. Table 3 shows the variations of hardness and elastic modulus as a function of pulsed parameter for the Zr films. The hardness values of the Zr films range from 4-8 GPa. Nanoindentation measurement indicate that the hardness of the film was about 6-8 GPa as a function of pulse frequency and duty cycle variation.

Table 3 Hardness and Elastic Modulus variation as a function of pulse parameters

| Parameters | | Hardness ±1(GPa) | Elastic Modulus ±20(GPa) |
|--------------|-----|---------------------|--------------------------------|
| Freq. (kHz) | 50 | 4.87 | 155.17 |
| | 100 | 6.40 | 198.67 |
| | 200 | 6.57 | 153.45 |
| Duty Cycle % | 10 | 6.15 | 162.39 |
| | 20 | 6.40 | 198.67 |
| | 30 | 6.42 | 170.81 |
| Power (W) | 50 | 7.8 | 205.6 |
| | 100 | 6.40 | 198.67 |

IV DISCUSSIONS

A. Effect of Pulse Power Supply Parameters on the Growth Characteristics

The crystallite size and deposition rates of Zr films are significantly influenced by some of the pulse parameters reported in the present work.

The deposition process is usually carried out with pulse frequencies (f_P) in the range 50-250 kHz. Increasing the pulse frequency increases the bombardment of target by high energy Ar atoms [23], leading to increased flux of sputtered atoms [24], which results in the decrease in the surface mobility of these species. As a consequence there is a reduction in the crystallite size. The growing film is bombarded by ions of appropriate energy to cause modification of its structure and properties, and the rate of arrival of the ions, and hence the degree of structural modification can be controlled by varying the pulse frequency. Also, the average power dissipated at the target decreases with increasing pulse frequency and at the start of each pulse there is a dead time during which negligible sputtering occurs and the proportion of this dead time increases with increasing pulse frequency and so the deposition rate is lower at a higher frequency [23,25]. The rate of voltage change at the target during the initial stages of the pulse-on period and the maximum negative voltage attained during the pulse-on period is significantly lower at higher frequencies [25]. Since sputtering rate is proportional to power and sputtering yield is proportional to target voltage, both these factors tend to lower the deposition rate at a higher frequency (Fig. 1(b)).

Pulse width is related to the duty cycle of the pulse and it is indirectly related to pulse frequency also. Duty cycle of any pulse can be defined as the ratio of on time of the pulse (pulse width) to the total time (on and off time) of the pulse. Duty cycle is the proportion of time during which electrical power source is operated. It controls the discharge duration of a single pulse and increasing the duty cycle at constant power increases the deposition rate (Fig. 5(b)). Duty cycle may provide a useful means for controlling film compositions. This is due

to the fact that the duty cycle determines the sputtering duration on each target and the amount of sputtered species. At higher duty cycle, the time for sputtering increases, which reduces the time for discharge for the accumulated species on the target and as a consequence the mobility of the accumulated species in the substrate decreases which leads to a decrease in the crystallite size as seen in the Fig. 5(c).

High pulse power in the magnetron sputtering process creates highly energized Ar ions which imparts kinetic energy to the sputtered atoms. Therefore the surface diffusion of these species is then enhanced on the growing surface, which leads to increased crystalline size. Also, the average power dissipated at the target increases with increasing pulse power which increases the deposition rate of the film as seen in Fig. 8(b). The XRD analysis of the Zr films with varying sputtering power indicated mixed orientation. It may be interpreted on the basis of stress present the film with increasing film thickness. The compressive stress induced in the films contributes to the development of (1 0 1) orientation and it may have relaxed to tensile mode at higher thickness (obtained with higher power) favoring the (0 0 2) preferred orientation.

B. Nanohardness of Zr thin films

Possible explanations for the larger hardness in the Zr films at $T_s=773$ K are a combination of smaller grain size, texture strengthening [26] and a nano-size effect, which is discussed in the following. The dependence of hardness on grain size agrees well with the well-known Hall–Petch [27-28] relation as

$$H = H_0 + KHd^{-1/2}$$

where H is the hardness, d being the average grain diameter, KH being the slope of the straight line drawn through the data, and H_0 is the intercept of the line with the coordinate axis. However no change in hardness value was observed with respect to pulsed parameters such as pulse frequency and duty cycle due to small variation in the crystallite size within the range of investigation. A slight increase in the hardness value as

a function of pulse power may be related with lower crystallites at low pulse power.

V. CONCLUSION

Formation of α -phase of zirconium with (002) preferred orientation was noticed at 773 K as a function of pulse parameter. It was found that crystallite size decreases with increasing frequency and duty cycle, whereas crystallite size increases with increasing pulse power. Nanoindentation measurements indicated that the hardness of the films is in the range 4-8 GPa. With proper pulse parameter selection it was noticed that well grown crystallites with α -hcp phase of zirconium at 773 K and 100 kHz, 20%, 100W of pulse frequency, duty cycle, pulse power respectively.

ACKNOWLEDGEMENT

The authors are thankful to Smt. M. Jyothi and Dr. Ramaseshan for their help in XRD and nanoindentation study. They are also grateful to Dr. M. Vijayalakshmi, AD, PMG, Dr. T. Jayakumar, Director, Metallurgy and Materials Group and Dr. Vasudev rao, Director, IGCAR for the support and encouragement.

REFERENCES

- [1] H.O. Pierson, New Jersey, USA, 1996, 181.
- [2] S. Ramanathan, C.M. Park, P.C. McIntyre, J. Appl. Phys. 91 (2002) 4521.
- [3] S. Niyomsoan, W. Grant, D.L. Olson, B. Mishra, Thin Solid Films 415 (2002) 187.
- [4] S. Miyazaki, M. Narasaki, M. Ogasawara, M. Hirose, Solid State Electron. 46 (2002) 1679.
- [5] N.L. Zhang, Z.T. Song, Q. Wan, Q.W. Shen, C.L. Lin, Appl. Surf. Sci. 202 (2002) 126.
- [6] H.M. Benia, M. Guemaz, G. Schmerber, A. Mosser, J.C. Parlebas, Appl. Surf. Sci. 200 (2002) 231.
- [7] L.Q. Shi, G.Q. Yan, J.Y. Zhou, S.Z. Luo, S.M. Peng, W. Ding, X.G. Long, J. Vac. Sci. Technol. A 20 (2002) 1840.
- [8] L.E. Toth, Transition Metal Carbides and Nitrides. Academic Press, New York, (1971).
- [9] L. Pichon, T. Girardeau, F. Lignou, A. Straboni, Thin Solid Films 342 (1999) 93.
- [10] M. Balaceanu, T. Petreus, V. Braic, C.N. Zoita, A. Vladescu, C.E. Cotrutz, M. Braic, Surf. Coat. Technol. 204 (2010) 2046.
- [11] A. Baudry, P. Boyer, M. Brunel, J. Magn. Mater. 185 (1998) 309.
- [12] D.J. Li, M.X. Wang, J.J. Zhang, Mater. Sci. Eng. A 423 (2006) 116.
- [13] L. Smardz, J. Alloys Compd. 395 (2005) 17.
- [14] Kendall J. Hollis, International Thermal Spray & Surface Engineering, Editors, Robert Gansert, William Jarosinski, Nov. 2010, 5 (4).
- [15] F. Abbasi, G.R. Etaati, H. Afarideh, R. Koohi-Fayegh, G.R. Aslani, Iranian J. Phys. Res. 3, No.2. (2002) 101.
- [16] F. Abbasi Davani, R. Koohi Fayegh, H. Afarideh, G.R. Etaati, G.R. Aslani, Radiation Measurement 37 (2003) 237.
- [17] J.P. Biersack, L.G. Haggmark, Nuclear Instrum. Methods Phys. Res. 174 (1980) 257.
- [18] SIMBAD - Thin Film Process Simulator. #318, 11315-87 Avenue, Edmonton, Alberta, Canada T6G 2T9: Alberta Microelectronic Center, 1997.
- [19] S. Schiller, K. Goedicke, J. Reschke, V. Kirchhoff, S. Schneider, F. Milde, Surf. Coat. Technol. 61 (1993) 331.
- [20] H. Ohsaki, Y. Tachibana, J. Shimizu, T. Oyama, Thin Solid Films 281/282 (1996) 213.
- [21] A. Singh, P. Kuppasami, R. Thirumurugesan, R. Ramaseshan, M. Kamruddin, S. Dash, V. Ganesan, E. Mohandas, Appl. Surf. Sci. 257 (2011) 9909.
- [22] J.L. Loubet, J.M. Georges, O. Marchesini, G. Meille, ASME J. Tribol. 106 (1984) 43.
- [23] Y.T. Pei, C.Q. Chen, K.P. Shaha, J.Th.M. De Hosson, J.W. Bradley, S.A. Voronin, M. Cada, Acta Mater. 56 (2008) 696.
- [24] Y.T. Pei, K.P. Shaha, C.Q. Chen, R. van der Hulst, A.A. Turkin, D.I. Vainshtein, J.Th.M. De Hosson, Acta Mater. 57 (2009) 5156.
- [25] P.J. Kelly, A.A. Onifade, Y. Zhou, G.C.B. Clarke, M. Audronis, J.W. Bradley, Plasma Processes Polym. 4 (2007) 246.
- [26] S.E. Hsu, G.R. Edwards, J.C. Shyne, O.D. Sherby, J. Mater. Sci. 12 (1977) 131.
- [27] E.O. Hall, Proc. Phys. Soc. Lond., B 64 (1951) 747.
- [28] N.J. Petch, J. Iron Steel Inst. 174 (1953) 25.